



# The excited states of $\text{Sr}^+\text{CO}$ : photofragmentation spectra and ab initio calculations

S.C. Farantos<sup>a,b,\*</sup>, E. Filippou<sup>a,b</sup>, S. Stamatiadis<sup>a</sup>, G.E. Froudakis<sup>b</sup>,  
M. Mühlhäuser<sup>c</sup>, M. Peric<sup>d</sup>, M. Massaouti<sup>a,b</sup>, A. Sfounis<sup>a,b</sup>, M. Velegrakis<sup>a</sup>

<sup>a</sup> *Institute of Electronic Structure and Laser, Foundation for Research and Technology Hellas, Iraklion, Crete 711 10, Greece*

<sup>b</sup> *Department of Chemistry, University of Crete, Iraklion 71110, Crete, Greece*

<sup>c</sup> *Institut für Physikalische und Theoretische Chemie der Universität Bonn, Wegelerstrasse 12, 53115 Bonn, Germany*

<sup>d</sup> *Faculty of Physical Chemistry, University of Belgrade, Studentski trg 12-16, P.O. 137, 11000 Belgrade, Yugoslavia*

Received 5 June 2003; in final form 4 August 2003

Published online: 10 September 2003

## Abstract

The first absorption band in the photofragmentation spectroscopy of  $\text{Sr}^+\text{CO}$ , is recorded in the energy region between 15 600 and 16 200  $\text{cm}^{-1}$ . The spectrum is characterized by a sharp peak between two zones with broad peaks. In contrast to this, the second absorption band observed in the energy interval of 19 000–23 000  $\text{cm}^{-1}$  shows a regular vibrational structure accompanied by a low intensity shoulder which covers the energy up to the dissociation. Electronic multi-reference configuration interaction calculations in the 2-D nuclear configuration space with the CO bond frozen provide a qualitative explanation of the spectra.

© 2003 Elsevier B.V. All rights reserved.

## 1. Introduction

The optical absorption spectra of  $\text{Sr}^+\text{CO}$  have been measured by photofragmentation spectroscopy of mass selected ions. The  $\text{Sr}^+(\text{CO})_n$  clusters were formed in a molecular beam apparatus via the injection of a plasma plume produced by a laser ablation of a Sr target into a supersonic expansion of CO gas into vacuum. After the separation of  $\text{Sr}^+\text{CO}$  cation with a mass gate, using a

tunable OPO laser system absorptions were recorded in the energy range of 15 600–16 200  $\text{cm}^{-1}$  and in the region of 19 000–23 000  $\text{cm}^{-1}$ . The first band is attributed to transitions from the ground electronic state to the states associated with  $4^2\text{D}$  manifold of strontium cation, and the second one is due to transitions to the  $5^2\text{P}$  states of strontium.

$\text{Sr}^+$  in its ground electronic state has one electron in the 5s orbital, hence a  $2\Sigma$  state in the  $C_{\infty v}$  symmetry group of  $\text{Sr}^+\text{CO}$ . The first excited atomic states are the  $4^2\text{D}$  which are split into one  $2\Sigma$ ,  $2\Pi$  and  $2\Delta$ , and the  $5^2\text{P}$  which are split into one  $2\Sigma$  and  $2\Pi$ . The experimentally recorded spectra are presented in Fig. 1. These two spectra

\* Corresponding author. Fax: +30-81-39-1305.

E-mail address: [farantos@iesl.forth.gr](mailto:farantos@iesl.forth.gr) (S.C. Farantos).

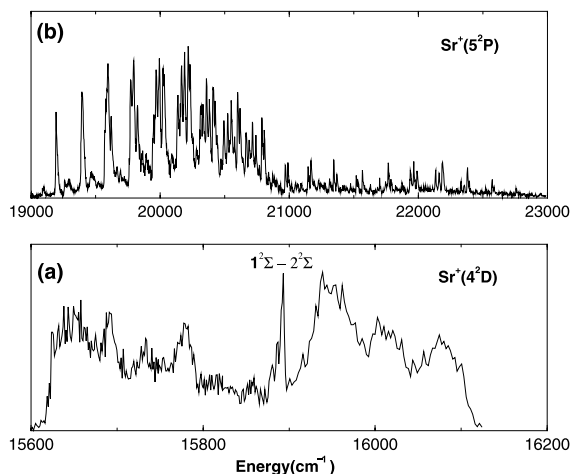


Fig. 1. The optical absorption spectra of  $\text{Sr}^+\text{CO}$  for transitions from the ground electronic states to the manifold of states originated from the  $\text{Sr}^+(4^2\text{D})$  (a) and  $\text{Sr}^+(5^2\text{P})$  (b) (see text).

are remarkably different, although both show bands with some vibrational structure. The low energy spectrum, Fig. 1a, consists of two zones with broad peaks and a sharp peak between, and it spans an energy interval of about  $500\text{ cm}^{-1}$ . The high energy spectrum, Fig. 1b, shows sharp regular progressions separated by approximately  $200\text{ cm}^{-1}$ , in an energy interval of  $4000\text{ cm}^{-1}$ . The most characteristic feature of Fig. 1b is the decrease of the intensity from  $21\,000$  to  $23\,000\text{ cm}^{-1}$ .

For a system such as  $\text{Sr}^+\text{CO}$  several phenomena contribute to the complexity of the spectrum. These are the spin–orbit and the non-adiabatic, Renner–Teller, splitting of the  $^2\Pi$  states. For the latter, the twofold electronic degeneracy for linear configurations of the nuclei is lifted in triangular geometries and two separate adiabatic potential energy surfaces dictate the dynamics of the complex. In the  $C_s$  symmetry group the two states give  $A'$  and  $A''$  irreducible representations, respectively. To find out the morphologies of the potential energy surfaces (PES), electronic structure calculations are required. Finally, although we cannot determine the temperature of the initially formed clusters some hot bands are expected and these could explain the small peaks that appear among the main ones in Fig. 1b.

In a recent article [1] (herein referred to as letter D) we dealt with the high energy spectrum of

$\text{Sr}^+\text{CO}$ ,  $1^2\Sigma \rightarrow 2^2\Pi$ . We carried out electronic configuration interaction calculations to produce potential energy surfaces as functions of the  $\text{Sr}^+\text{CO}$  stretch and bend coordinates with the CO bond length frozen. These calculations revealed the existence of a bistable species with strontium either bonded to the carbon-end or to the oxygen-end of CO in collinear geometries. Furthermore, by solving the time dependent Schrödinger equation and employing single adiabatic PES, we simulated the vibrational spectrum. We showed that the progressions observed are mainly due to Sr–C and Sr–O stretch overtones. However, in order to explain the broadness of the low intensity shoulder it was necessary to accept excitations of the  $\text{Sr}^+\text{CO}$  bend mode as well.

In the present Letter we mainly concentrate in the study of the low energy spectrum of  $\text{Sr}^+\text{CO}$ ,  $1^2\Sigma \rightarrow 1^2\Pi$ . In spite of its short range ( $500\text{ cm}^{-1}$ ) which makes a quantitative agreement with the ab initio calculations difficult, the theoretical results can elucidate the main spectral features.

## 2. Results and discussion

The time of flight apparatus as well as experimental details were presented in previous publications [2]. Also, in letter I we described in detail the ab initio electronic structure calculations. Here, for completeness, we give a brief description of the methods and basis sets employed.

The computations of the electronically excited states were performed with the multi-reference single- and double-excitation configuration interaction method, MR-CI, implemented in the Molpro 2000 package of programs [3]. The contribution of higher excitations is estimated by applying a generalized Langhoff–Davidson correction formula.

The MR-CI calculations are performed in the Abelian subgroup  $C_{2v}$  for collinear geometries and  $C_s$  for triangular geometries. As (multi-)reference space we have chosen all possible configurations which can be created in each irreducible representation within an active space of nine  $\sigma$  orbitals and three  $\pi$  orbitals. The number of reference configurations per irreducible representation was

in the range of nine  $A'$  and five  $A''$ . An analysis of the molecular orbitals (MO) involved in these reference configurations justified the prior choice of the active space.

Moreover, the geometry of  $\text{Sr}^+\text{CO}$  in the ground electronic state has been fully optimized using spin-restricted singles and doubles coupled cluster calculations with a perturbative inclusion of the connected triple excitations RCCSD(T).

For carbon and oxygen we used the correlation-consistent triple zeta basis set of Dunning [4–7] augmented by two d- and one f-polarization functions. For strontium atom we used the 10-valence-electron quasi-relativistic effective core potential (ECP) from the Stuttgart group [8] in conjunction with the correlation-consistent triple zeta basis set of Dunning [4–7]. The chosen basis set is flexible with respect to polarization and electronic correlation and is considered to be fairly balanced for all states treated.

Using Jacobi coordinates, the vector  $\vec{R}$  from the center-of-mass of CO to  $\text{Sr}^+$ , the vector  $\vec{r}$  joining the nuclei C and O the length of which is kept fixed at 1.201 Å, and the angle  $\gamma$  between them, we computed the PES in the  $(R, \gamma)$  plane in the range of  $R = 2\text{--}5$  Å and  $\gamma = 0\text{--}180^\circ$  for all states pertinent to the spectra. The total grid comprised 31 distances and 19 angles. Furthermore, we have fitted the ab initio points by analytical potential energy surfaces as series in a bicubic B-spline expansion. Routines from the NAG library [9] are used which combine the spline representation with a least square fit for finding the coefficients in the expansion. The root mean square deviations are from 0.01 to 0.1 eV.

Instead of showing contour plots of the adiabatic PES, for the purpose of this Letter it is more useful to plot potential curves as functions of the Jacobi angle  $\gamma$ , minimizing the energy with respect to  $R$ , (Fig. 2b), and the bond length of  $\text{Sr}^+\text{--C}$ , for  $\gamma = 0$ , Fig. 2a. In Table 1 we tabulate the equilibrium bond lengths, binding energies, vertical transitions and dissociation limits for the carbon-bonded isomer. All energies are measured with respect to the dissociation limit of the ground electronic state,  $\text{Sr}^+(5^2\text{S}) + \text{CO}(1^1\Sigma^+)$ , for which the zero energy is defined. Similar data for  $\text{Sr}^+$  collinearly approaching the O end of CO were presented in letter I.

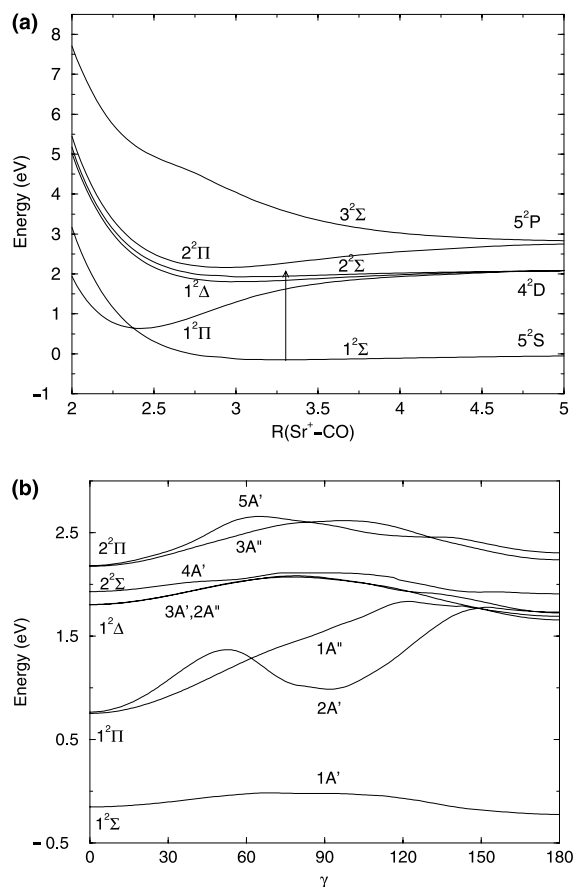


Fig. 2. (a) Potential energy curves for  $\text{Sr}^+$  coaxially approaching the carbon atom. (b) The minimum energy paths in the potential energy surfaces of  $\text{Sr}^+$  moving around CO.  $\gamma = 0$  corresponds to the carbon side, and  $\gamma = 180^\circ$  to the oxygen side. The zero of energy is defined for the dissociation limit,  $\text{Sr}^+(5^2\text{S}) + \text{CO}(1^1\Sigma^+)$ . The arrow denotes the vertical transition from the equilibrium geometry of the ground electronic state to the  $^2\text{D}$  manifold of states.

In the last column of Table 1 we compare the calculated dissociation limits with the experimental excited states of  $\text{Sr}^+$  [10]. We see that the  $4^2\text{D}$  states are overestimated by 0.3 eV whereas the  $5^2\text{P}$  states are underestimated by 0.1 eV. The calculations reveal linear absolute and relative minima for all states except the repulsive  $3^2\Sigma$ . In the ground electronic state the binding energies are 0.15 and 0.21 eV for the carbon-bonded and oxygen-bonded isomer, correspondingly. Thus, the binding of strontium to the oxygen side results in a slightly

Table 1

Strontium–carbon equilibrium bond lengths ( $r_e$ ), binding energies ( $E_b$ ), vertical transitions ( $T_c$ ) and dissociation energies ( $E_d$ ) for  $\text{Sr}^+ - \text{CO}$

State	$r_e$	$E_b$	$T_c$	$E_d$
$1^2\Sigma^+$	3.31	0.149	–	0
$1^2\Pi$	2.42	1.510	1.781 (1.937) <sup>a</sup>	2.146 (1.805 $4^2D_{3/2}$ ) <sup>b</sup> (1.839 $4^2D_{5/2}$ ) <sup>b</sup>
$1^2\Delta$	3.10	0.198	1.992	2.132
$2^2\Sigma^+$	3.12	0.226	2.094 (1.971) <sup>a</sup>	2.154
$2^2\Pi$	2.96	0.666	2.423 (2.380) <sup>c</sup>	2.830 (2.940 $5^2P_{1/2}$ ) <sup>b</sup> (3.040 $5^2P_{3/2}$ ) <sup>b</sup>
$3^2\Sigma^+$	–	–	3.704	2.815

The zero energy corresponds to  $\text{Sr}^+(5^2S) + \text{CO}(1^1\Sigma^+)$  with calculated energy  $-143.239223$  Hartree. Energies are in eV and distances in Å. The distance of CO was kept fixed at 1.201 Å. The numbers in parentheses are experimental results.

<sup>a</sup>The first high intense peak in the spectrum of Fig. 1a.

<sup>b</sup>Excitation energies of  $\text{Sr}^+$  from [10].

<sup>c</sup>The first high intense peak in the spectrum of Fig. 1b.

more stable complex. On the other hand, in the  $1^2\Pi$  state originated from the  $4^2D$  manifold of  $\text{Sr}^+$ , the binding energies are 1.51 eV for the C-bonded and 0.62 eV for the O-bonded isomer. The vertical transitions from the equilibrium geometries of both isomers in the ground electronic state to  $1^2\Pi$  state are 1.781 and 1.928 eV for the relative and the absolute minima, respectively. The numbers in parentheses (Table 1) are the energies of the first intense peak in Fig. 1. The bond length of CO in the ground electronic state of  $\text{Sr}^+\text{CO}$  complex was found to be 1.201 Å, which is larger than the bond length of the free molecule (1.128 Å). Energetic and geometrical characteristics for all PES are given in Tables 1 and 2 of letter I.

Table 2

Energies and symmetries of the vibronic levels in the  $1^2\Pi$  state of  $\text{Sr}^+\text{CO}$

$v_b$	$K_{S_z}$	$E$ ( $\text{cm}^{-1}$ )
1	$\Sigma_{\pm 1/2}$	570
1	$\Delta_{5/2}$	537
2	$\Pi_{3/2}$	530
2	$\Pi_{1/2}$	529
2	$\Phi_{5/2}$	490
0	$\Pi_{3/2}$	352
1	$\Sigma_{\pm 1/2}$	289
1	$\Delta_{3/2}$	280
0	$\Pi_{1/2}$	67

$v_b$  denotes the bending vibrational quantum number and  $K_{S_z}$  the projection of the total angular momentum on the  $z$ -axis.

We immediately notice from Fig. 2a the large contraction of the equilibrium bond length of  $\text{Sr}^+ - \text{C}$  in the  $1^2\Pi$  state. Absorptions are dipole moment allowed to  $1^2\Pi$  and to the  $2^2\Sigma$  state but not to the  $1^2\Delta$  state. From Table 1 we estimate the energy difference between dissociation and the vertical transition in the  $1^2\Pi$  state to be 0.37 eV, i.e., comparable to the difference between the calculated dissociation energy and experimentally observed energies of strontium cation. This deprives us of a quantitative comparison with the experimental spectrum. Nevertheless, the potential curves do predict excitations close to the dissociation limit which justifies the short absorption bands observed in spite of the deep minimum of the  $1^2\Pi$  state. We also notice the crossing of this state with the electronic ground state near the equilibrium geometry. Excitations from the isomer  $\text{Sr}^+\text{OC}$  are predicted to be even closer to the dissociation limit (1.928 eV) according to our calculations.

The decreasing intensities in the first zone of the recorded spectrum is in accord with a dissociating species. In order to explain the other features of the spectrum, a sharp peak and the second broad zone which indeed shows a similar pattern as the first one, we must study the spin–orbit and Renner–Teller interactions. These require us to investigate the role of the bending motion in the complex. In Fig. 2b the minimum energy paths are

depicted for the isomerization  $\text{Sr}^+\text{CO} \rightarrow \text{Sr}^+\text{OC}$  computed for the electronic states in question. We have assigned the potential curves according to the  $C_s$  symmetry group. For linear geometries we expect the  $2A'$  and  $1A''$  states to become degenerate,  $1^2\Pi$ . The same with the PES associated with the  $1^2\Delta$  and  $2^2\Pi$  states. In good approximation the degeneracy is satisfied for the  $\text{Sr}^+\text{CO}$  ( $\gamma = 0^\circ$ ), but to a lesser extent for its isomer  $\text{Sr}^+\text{OC}$  ( $\gamma = 180^\circ$ ).

The energy difference between the  $2A'$  and  $1A''$  states dictates a moderate non-adiabatic interaction for the  $1^2\Pi$  state, whereas for the  $1^2\Delta$  state the splitting is negligible. These features enable simple computations for the vibronic structure accompanied with the spin–orbit coupling in the framework of the perturbation theory. Such a theory has been recently presented for the  $2^2\Pi$  and  $2^2\Delta$  states [11,12].

The harmonic bending vibrational frequency  $\omega$  for the mean potential  $\frac{1}{2}(V^+ + V^-)$ , where  $V^+$  and  $V^-$  are the adiabatic potentials for the  $2A'$  and  $1A''$  states, is estimated to be  $220 \text{ cm}^{-1}$ . Thus, it is comparable in magnitude with the spin–orbit coupling constant of Sr, which is about  $A = 300 \text{ cm}^{-1}$  (see [10]). In the frame of perturbation theory the vibronic energy levels are distinguished into two classes according to the quantum number  $K$ , the projection of the total angular momentum excluding spin on the  $z$ -axis. The first class corresponds to  $K = v_b + 1$  and are given by [11]:

$$E = (v_b + 1)\omega + S_z A - \frac{1}{8}\epsilon^2\omega^2 \frac{K(K+1)}{(\omega - S_z A)}, \quad (1)$$

where  $v_b$  is the bending quantum number and  $S_z$  is the quantum number for the projection of the spatial and spin electronic angular momentum on the  $z$ -axis.  $\epsilon$  is the Renner dimensionless parameter computed to be 0.321. All other vibronic levels are given by the formula:

$$E_{1/2} = (v_b + 1)\omega \pm S_z A - \frac{1}{8}\epsilon^2\omega^2 \left[ \frac{(v_b \mp K + 1)(v_b \mp K + 3)}{4(\omega \pm S_z A)} - \frac{(v_b \pm K)^2 - 1}{4(\omega \mp S_z A)} \pm \frac{(v_b + 1)^2 - K^2}{S_z A} \right]. \quad (2)$$

Employing these formulae we obtain the vibronic levels up to  $600 \text{ cm}^{-1}$  tabulated in Table 2. Assuming that only the lowest vibrational level of the ground electronic state,  $1^2\Sigma$ , is populated, the vibronic transitions to  $K = 0$  (parallel bands) and  $K = 1$  (perpendicular bands) of the  $1^2\Pi$  electronic state are allowed. The latter are expected to be generally at higher intensity, which are non-vanishing at linear geometry. The most intense bands should correspond to the unique  $\Pi(K = 1)$  levels, computed at  $67$  and  $352 \text{ cm}^{-1}$ . These two bands should be separated by approximately  $300 \text{ cm}^{-1}$ , being the assumed value of spin–orbit constant. Among the parallel transitions only that involving the  $\Sigma_{\pm 1/2}$  levels at  $289 \text{ cm}^{-1}$  lies in the energy range where the spectrum was observed.

According to these calculated energies we may conclude that the first zone is due to transitions from the ground state to the  $v_b = 0$  vibronic state, and the second zone may be attributed either to the second bending vibronic level  $v_b = 1$  ( $\Sigma_{\pm 1/2}$ ) or to the second spin–orbit component in its ground vibronic level ( $\Pi_{3/2}$ ). The structure observed in each zone is most likely vibrational levels of the  $\text{Sr}^+\text{C}$  stretch mode close to the dissociation limit.

The bending frequency for the  $2^2\Sigma$  state is computed to be  $120 \text{ cm}^{-1}$ , i.e., very similar to that of the ground electronic state. From Fig. 2b we can see that the potential curves of the ground electronic state,  $1^2\Sigma$ , and the  $2^2\Sigma$  are almost parallel. Thus, mainly one transition between the lowest vibrational levels is expected and that explains the sharp peak in the spectrum.

Finally, the splitting of the  $1^2\Delta$  state ( $3^2A'$ ,  $2^2A''$ ) is negligible (Fig. 2b), and therefore, the spin–orbit splitting dominates in these states. It is not expected, however, that the  $2^2\Delta$  state contributes appreciably to the spectrum, because the electronic transition from the ground state is forbidden at linear geometries. On the other hand, the  $2^2\Delta$  state may play an indirect role through its interaction with the other members of the  $4^2D$  manifold at non-linear nuclear arrangements, as is seen in the region around  $\gamma = 180^\circ$ , Fig. 2b. However, it is more likely that excitations from the oxygen bonding isomer lead to dissociation, and thus, they are not recorded in the spectrum.

### 3. Conclusions

In this paper we investigate the spectral features of the first absorption band in the electronic excitations of  $\text{Sr}^+\text{CO}$  by carrying out ab initio quantum chemical calculations with the multi-reference configuration interaction method. Transitions are recorded in the energy interval of 15 600–16 200  $\text{cm}^{-1}$ . The small energy absorption window requires very accurate calculations. With the existing effective core potential for strontium it turns out that it is not possible to reach this level of accuracy. However, our theoretical results give a qualitative answer which seems to be in accord with the spectral features observed. Potential energy surfaces for the ground as well as the  $4^2\text{D}$  states of strontium involved in the transitions  $1^2\Sigma \rightarrow 1^2\Pi$  and  $1^2\Sigma \rightarrow 2^2\Sigma$  have been computed as functions of the stretch and bend coordinates of  $\text{Sr}^+\text{CO}$ . Their topographical characteristics in association to a perturbative estimate of the vibronic levels in the  $1^2\Pi$  state helped us to draw the following conclusions:

- (i) The narrow absorption window is explained because of the large displacement of the equilibrium geometries between the ground and the first excited state,  $1^2\Pi$ , which brings the complex close to the dissociation limit. Excitations from the oxygen bonded isomer although predicted by our calculations are not observed, most likely because they excite the complex above dissociation.
- (ii) The two broad zones correspond to the two spin–orbit interaction surfaces which are expected to run parallel with the angle coordinate. However, the first bending excitation could be hidden in the second zone. The structure observed in each zone is attributed to stretching vibrations of  $\text{Sr}^+\text{C}$ .
- (iii) The sharp peak between the two zones results from the  $1^2\Sigma$  to  $2^2\Sigma$  transition since no substantial displacement in the equilibrium geometries is found for these states.

- (iv) Finally, since a transition to  $1^2\Delta$  state is not allowed for collinear geometries, the direct participation of this state to the recorded spectrum is limited.

### Acknowledgements

We are grateful to Professor S.D. Peyrimhoff for many stimulating discussions. The theoretical study presented is part of a Greek–German collaborative linkage grant DAAD Program Griechenland IKYDA 2001'. Support from the Ministry of Education and European Union through the post-graduate program EPEAEK, Applied Molecular Spectroscopy', and the European Ultraviolet Laser Facility (Project: HPRI-CT-1999-00074) operating at FORTH are gratefully acknowledged.

### References

- [1] S.C. Farantos, E. Filippou, S. Stamatidis, G.E. Froudakis, M. Mühlhäuser, M. Massaouti, A. Sfounis, M. Velegarakis, *Chem. Phys. Lett.* 366 (2002) 231.
- [2] G.S. Fanourgakis, S.C. Farantos, Ch. Lüder, M. Velegarakis, S.S. Xantheas, *J. Chem. Phys.* 109 (1998) 108.
- [3] MOLPRO 2000 is a package of ab initio programs written by H.-J. Werner, P.J. Knowles and contributors.
- [4] D.E. Woon, T.H. Dunning Jr., *J. Chem. Phys.* 100 (1994) 2975.
- [5] D.E. Woon, T.H. Dunning Jr., *J. Chem. Phys.* 98 (1993) 1358.
- [6] R.A. Kendall, T.H. Dunning Jr., R.J. Harrison, *J. Chem. Phys.* 96 (1992) 6796.
- [7] T.H. Dunning Jr., *J. Chem. Phys.* 90 (1989) 1007.
- [8] M. Kaupp, P.v.R. Schleyer, H. Stoll, H. Preuss, *J. Chem. Phys.* 94 (1991) 1360.
- [9] Nag\_spline\_2d, Nag\_spline\_2d\_lsq\_fit, *NAG Fortran 90 library*, Release 4, The Numerical Algorithms Group Ltd., Oxford, 2000.
- [10] C.E. Moore, *Atomic Energy Levels* (Natl. Bur. Stand., 1949), Circular 467, vol. I, p. 192.
- [11] M. Perić, S.D. Peyerimhoff, *J. Mol. Spectrosc.* 212 (2002) 142.
- [12] M. Perić, S.D. Peyerimhoff, *J. Mol. Spectrosc.* 212 (2002) 153.